Growth Kinetics of Vitamin C Crystals in a Batch L(+)-Ascorbic Acid–Methanol–Ethanol–Water System: Size Independent Growth Model Approach

B. Wierzbowska,[a] K. Piotrowski,[b,*] J. Koralewska,[a] and A. Matynia[a]
[a]Faculty of Chemistry, Wroclaw University of Technology, Wybrzeze Wyspianskiego 27, 50 – 370 Wroclaw, Poland
[b]Department of Chemical & Process Engineering, Silesian University of Technology, ks. M. Strzody 7, 44 – 101 Gliwice, Poland

Original scientific paper
Received: May 30, 2007
Accepted: January 30, 2008

The experimental data concerning growth kinetics of vitamin C (L(+)-ascorbic acid, LAA) crystals in a seeded and cooling batch mass crystallization process realized in a four–compound: L(+)-ascorbic acid–methanol–ethanol–water system are reported. Influences of initial composition of solution and its linear cooling rate on "average, effective" values of crystal linear growth rate were examined. Small divergences between LAA crystal size distributions (CSDs) data from granulometric analysis and Coulter counter were interpreted theoretically and discussed. Linear growth rates of crystals in a batch crystallizer were acquired with a proposed by *Nývlt* indirect method, based on the analysis of population density $n(L)$ data in a MSMPR (*mixed suspension mixed product removal*) crystallizer. Size–independent growth (SIG) kinetics was assumed. It can be concluded, that the largest and the most uniform particles of purified, crystalline vitamin C correspond to higher initial concentration of L(+)-ascorbic acid in a solution and lower cooling rate applied.

Key words:
Vitamin C, methanol, ethanol, crystal growth kinetics, DT batch crystallizer, size-independent growth (SIG) kinetic model

Introduction

Vitamin C (L(+)-ascorbic acid, $C_6H_8O_6$, denoted later as LAA), a key ingredient of complex medicaments or multivitamins and natural antioxidant, is an essential compound of pharmaceutical and food industry products.[1] This organic compound influences fundamental metabolic functions of human organism, being responsible, among others, for the structural strength of the blood vessels, metabolism of selected aminoacids or oriented distribution of specific hormones.[2] According to a *Reichstein* procedure, LAA is synthesized from D-glucose.[3,4] However, average content of main product in a post-synthesis mixture in industrial conditions reaches only w = 96 – 98 % level.[5] Increase in chemical purity of LAA is acquired by means of sequencing batch crystallization/dissolution/recrystallization processes from its water solutions.[5–10] An essential inconvenience of the purification process is a relatively high number of the labour–consuming batch operations, favoring undesirable decomposition of LAA, which – demonstrating strong reducing properties[11] – is quickly oxidized in presence of atmospheric air. This side-process considerably lowers quality of crystal product removed from successive batch crystallization stages, being additionally catalyzed by higher temperature, lower pH and presence of active carbon, copper, iron or other heavy metals.[12–16] Introduction into the analyzed binary LAA–water system a third component – aliphatic alcohol (in practice one from C_1 – C_3) offers a new possibility of influencing the process yield and upgrading its quality by reduction of indispensable number of batch crystallization stages.[17,18] Alcohol(s) (individual or their mixture) presence effects in versatile physicochemical interactions within the discussed system, modifying solubility, metastable zone width as well as nucleation and growth rates of LAA crystals.[10,19,20]

Experimental data concerning linear growth rate of vitamin C (LAA) crystals in a four–compound: LAA–methanol–ethanol–water system are presented. The test measurements were carried out in a laboratory batch DT (*draft tube*) crystallizer of internal circulation of suspension with assumed cooling rate controlled precisely on-line by a PC computer system. Growth rates were estimated indirectly from the CSDs (*crystal size distributions*) of a batch process product, rearranged in a form of crystal population density functions.

The CSDs were determined with two methods: using laser particle size analyzer COULTER LS-230 and by means of conventional granulometric analy-

*Corresponding author: krzysztof.piotrowski@polsl.pl

sis (PN-67/M-94001). A kinetic model of continuous MSMPR (*mixed suspension mixed product removal*) crystallizer, mathematically convenient for the kinetic data determination was formally adopted for the estimation of "effective growth kinetics" in the batch process conditions. Values of linear growth rate of LAA crystals evaluated with the use of the most simplified kinetic model (*size-independent growth* – SIG) are presented. For the purpose of kinetic data elaboration the solubility and spontaneous nucleation temperature data presented in the authors' earlier work[21] were used.

Kinetics of crystals growth in the batch crystallization processes

Batch crystallization processes are especially convenient for the performance of laboratory experiments. However, in the continuous processes fixed or slightly oscillated within the pseudo steady-state limits the values of process temperature, supersaturation, suspension density, specific surface area of dispersed crystal phase, etc. guarantee temporal stability of resulting kinetic feedbacks inside the system, thus stabilized and physically grounded values of nucleation and growth rates. In batch systems both intrinsic complexity and essential differences in intensity of various partial processes in time occur. Appearance of a new solid phase, enlargement of mass and surface area of isolated crystal population while batch process course as well as dramatic time-variability of supersaturation result in a significant changeability of kinetic parameter values during the process run. Thus possibly precise and detailed enough physical model of a batch mass crystallization process requires simultaneous integration of a relatively complex system of time-dependent population, mass and energy balances, generally in a form of differential equations, complemented by appropriate kinetic dependencies.[22]

In the literature one can find original propositions of the batch kinetic data elaboration.[23–32] One of the mathematically convenient and relatively simple manners may be an indirect method proposed by *Nývlt*. It is based on the evaluation of G value from population density function derived from cumulative mass (or volume) CSD obtained in a batch crystallizer with mixer and programmed cooling, thus in a complex unsteady-state polythermic and induced (seeded) process of combined nucleation and crystal growth.[9,33,34]

Nývlt suggests[33] that in some process conditions mass CSD produced in a batch crystallizer and presented in a "$z - L$" coordinate system (see eqs. (1) and (2)):

$$W(z) = 1 - \left(1 + z + \frac{z^2}{2} + \frac{z^3}{6}\right)\exp(-z) \qquad (1)$$

$$z = \frac{L}{G\tau} \qquad (2)$$

where: W – normalized cumulative mass distribution (undersize), z – dimensionless size, is apparently a straight line – thus qualitatively similar in this coordinate system to a theoretical mass CSD coming from a continuous MSMPR crystallizer. It gives grounds for a formal assumption that the final equations derived from population balance corresponding to a continuous process and applied – formally exclusively – for this regime description can be practically used as a convenient mathematical tool for the elaboration of batch data, yielding in effect the conventional "substitute, effective, average" kinetic parameter values. Moreover, intensity of mixing observed by the authors during own batch experiments justifies formal assumption of MSMPR model as far as concerns the ideal mixing of suspension inside the crystallizer vessel (*mixed suspension*), while analysis of a whole final crystal product (total working volume of laboratory crystallizer creates here an "product suspension sample") is a formal and practical equivalent of its unclassified, representative removal (*mixed product removal*).

Eq. (3) representing the SIG (*size–independent growth*) kinetic model:[35]

$$n = n_0 \exp(-L/G\tau) \qquad (3)$$

where the individual population density values, n_i, can be calculated from mass $m(L)$ (or volume, $V(L)$) size distribution data according to the formula below, eq. (4):

$$n_i = \frac{m_i}{k_v \rho L_i^3 \Delta L_i V_w} = \frac{V_i}{k_v L_i^3 \Delta L_i V_w} \qquad (4)$$

can be thus – according to the method's assumptions – directly adopted for rough calculation of G value in a batch crystallization process by formal substitution of mean residence time, τ, with a batch crystallization time, t_{cr}, eq. (5) (see Fig. 1):

$$\tau \approx t_{cr} = \frac{T_{cr} - T_f}{R_T} + t_f \qquad (5)$$

This way t_{cr} value depends both on the physicochemical properties of initial solution introduced into batch crystallizer ($T_{cr} = T_s - \Delta T_{max}$, $\Delta w_{max} = (dw/dT)_{eq}\Delta T_{max}$) and on technological process conditions applied (R_T, T_f, t_f). Taking advantage of a $T_{cr} = T_s - \Delta T_{max} = f(w_{LAA}, w_{MeOH}, w_{EtOH})$

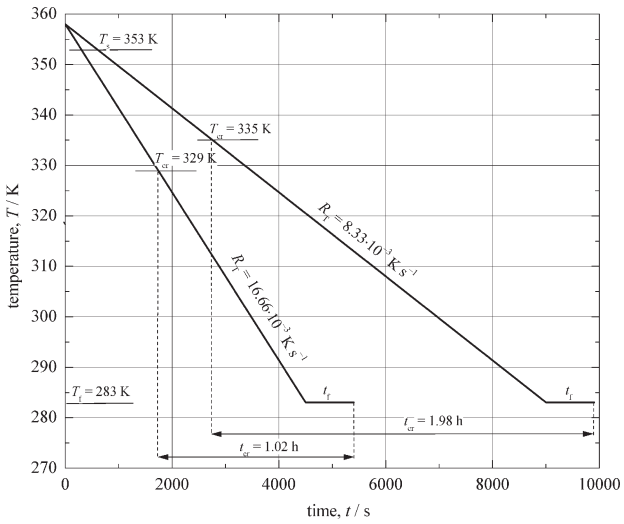

F i g . 1 – *Parameters of cooling process coupled with mass crystallization phenomena in a DT batch crystallizer – two batch process times for exemplary solution of initial composition: LAA – 50, MeOH – 10, EtOH – 10, H_2O – 30 % resulting from two values of linear cooling rate applied*

dependency evaluated earlier,[21] eq. (5) can be presented in a more detailed form of: $\tau \approx t_{cr} = f(w_{LAA}, w_{MeOH}, w_{EtOH}, T_f, R_T, t_f)$ – see eq. (5a):

$$\tau \approx t_{cr} = \frac{2.932 w_{LAA} + 0.671 w_{MeOH} + 0.883 w_{EtOH} + 174.78 - T_f}{R_T} + t_f \quad (5a)$$

It is, however, not a precise method since it is based on a formal assumption that granulometric composition of the final product, obtained in a very complex batch, non-isothermal and seeded process of nucleation coupled with crystals growth, during which both temperature and supersaturation are the subjects of dramatic changes, is theoretically identical with a product of continuous MSMPR crystallizer working in identical technological conditions assuming mean process temperature of the comparable batch run and excluding seeding.[36–38] The authors' own research experience suggests, that with this method one can only roughly estimate the – not closely defined – "average", "effective" crystal growth rate G (since in a batch mode it is strongly time-dependent value). The resulting kinetic data should be rather used to a general estimation of the production capacity and/or for some rough design calculations, applied *e.g.* as the nominal values.[33] The essence of the assumed theoretical simplification is evaluation of a conventional, entirely computational value – a parameter named "average effective linear growth rate" of crystals, G, producing in a complex batch process CSD identical with size composition of the product removed from a continuous MSMPR crystallizer of average residence time of suspension identical with the corresponded batch run time (assuming identical other technological conditions). From theoretical point of view each batch process configuration, including: assumed initial composition of solution, starting temperature of the process, fixed mode (eventually value) of cooling rate, batch process time, mass and average size (or size distribution) of seeds, etc. can be attributed to a such "average effective linear growth rate, G". Thus, this entirely computational value may find potential application in practice for quick engineering calculations, eventually recognized as a direct and instant indicator for comparison purposes (*reference index*) while examining various technological options of a batch crystallization process. Moreover, this value adequately represents and reflects a resulting "net-effect" of the complex hydrodynamic and kinetic conditions (nonlinearly changeable during the process time-course).

Experimental setup and procedure

Experimental setup

The research stand scheme is presented in Fig. 2. Experiments were performed in a laboratory batch DT crystallizer of V_w = 0.6 dm^3 working volume with internal circulation of solution/suspension. It was a hermetic, glass-made cylindrical tank (V_t = 1 dm^3, D = 120 mm, H = 123 mm) equipped with a cooling jacket (*pipe-in-pipe* type heat exchanger) embedded into a circulation profile element wall, coupled with thermostat, where an ice load was applied to cool the heat acceptor – circulating double distilled water – down to a T = 275 K value. Actual temperature in a crystallizer vessel was monitored by automatic system integrated with

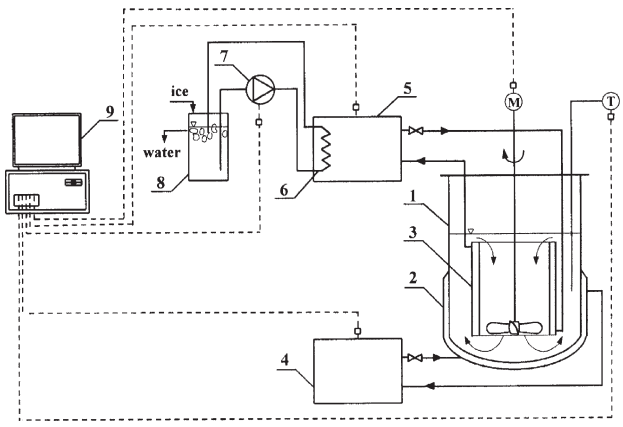

F i g . 2 – *Experimental setup of the laboratory batch crystallizer system: (1) DT MSMPR crystallizer with internal circulation of the solution/suspension, (2) heating jacket, (3) cooler, pipe-in-pipe type heat exchanger, (4) thermostat (heating), (5) thermostat (cooling), (6) cooling coil, (7) cooling medium pump, (8) cooling water tank: ice + distilled water, (9) PC computer, (M) stirrer speed control, (T) temperature control*

a PC computer, what enabled one to realize an assumed cooling mode, *e.g.* linear cooling profile with an accuracy of ± 0.7 K h^{-1}. In the tank axis, inside the circulation tube (DT) (d = 57 mm, h = 53 mm) a three-paddle propeller mixer (d_m = 55 mm) was installed. Revolution number was assumed constant[39] ($N = 10 \pm 0.2$ s^{-1}) providing stable and intensive enough circulation of solution (after nucleation – suspension) inside working volume.

Experimental procedure

The solutions of various compositions, as biochemically active materials, were prepared just before their insertion into the crystallizer using LAA of > 99.7 % purity (GR for analysis and for biochemistry, MERCK, Germany), double distilled water, MeOH (p., POCH Gliwice, Poland) and EtOH (p.a., 96 %, ZPS Polmos, Poland). The 0.7 kg of solution of known composition was heated till its actual temperature was ca. 5 K higher than the expected solubility temperature, T_s, roughly estimated on the basis of preliminary test results[21,39] – see Fig. 1. In this moment internal circulation of mixture started. After ca. 15 min of this isothermal circulation the cooling process began with a constant cooling rate, R_T, programmed by a computer driven automatic control system. When the solution reached a temperature 1 K lower than the expected solubility temperature, T_s,[21] thus crossed lower boundary of metastable zone, dozens of well shaped LAA crystals[36,38] were introduced into the mixed system (ca. 0.1 g of total mass, L_s = 900 μm). Continuous observation of the cooled system was realized till a moment when characteristic nucleation event was attained, manifested as a sudden turbidity within the bulk solution. Corresponded temperature of suspension can be interpreted as the spontaneous crystallization temperature, T_{cr},[21,40] – a value necessary in eq. (5). When the system attained its assumed final temperature, T_f = 283 K, cooling process was terminated. The resulting, still circulated suspension, was stabilized isothermally in temperature T_f through the defined time t_f = 900 s. Then the product crystals were dewatered by a centrifugal separation process, washed with cold ethanol and dried in a temperature T = 298 K without light (photodecomposition prevention). CSD analysis of the crystal product was carried into effect using two different methods – Coulter counter test and a classical granulometric analysis procedure. The experiments covered influences of saturation temperature, T_s, of initial solution (thus its assumed composition)[21] and linear cooling rate, R_T, on "average, effective linear growth rate" G of LAA crystals.

Influence of saturation temperature

Influence of saturation temperature of the mixture, indirectly – solution's composition – on the growth kinetics, $G = f(T_s)$, was investigated assuming a selected, constant value of linear cooling rate, $R_T = 8.33 \cdot 10^{-3}$ K s^{-1}. Batch crystallizer was provided with solutions of the following compounds:

– w_{LAA} = 40, 45 and 50 %,

– $w_{MeOH} + w_{EtOH}$:

$12 \le w_{MeOH} + w_{EtOH} \le 40$ % for $w_{LAA} = 40$ %,

$12 \le w_{MeOH} + w_{EtOH} \le 30$ % for $w_{LAA} = 45$ %,

$12 \le w_{MeOH} + w_{EtOH} \le 20$ % for $w_{LAA} = 50$ %,

– double distilled water – a complement to 100 %.

The solutions of w_{LAA} = 45 or 50 % were mixed with lower fractions of MeOH+EtOH mixture than it was in case of w_{LAA} = 40 %. Higher fractions of alcohols caused undesired boiling of the solution within temperature range lower than LAA solubility temperature, T_s. The 27 diversified compositions of four-compound LAA–MeOH–EtOH–H_2O solutions were tested. For each mixture composition G value was determined on the basis of corresponded CSD data (in $n(L)$ form).

Influence of linear cooling rate

For three solutions, selected from 27 ones described above, of the following compositions (w/%):

– LAA – 40, MeOH – 10, EtOH – 10, water – 40 %,

– LAA – 45, MeOH – 10, EtOH – 10, water – 35 %,

– LAA – 50, MeOH – 10, EtOH – 10, water – 30 %,

additional tests were performed providing the system with a linear cooling rate elevated to a value of $R_T = 16.66 \cdot 10^{-3}$ K s^{-1} (see Fig. 1), resulting in a $G = f(t_{cr})$ relationship elaboration possible. These purposefully selected compositions can be of practical significance in pharmaceutical industry. Because presence of alcohol(s) in this system reduces the LAA solubility,[21] simultaneously reducing the solution's boiling temperature, in technological practice total fraction of MeOH+EtOH should not exceed w = 20 %.

For experimentally obtained original CSDs of product crystals from two independent sources: Coulter counter and granulometric analysis, population density courses $n(L)$ were computed with the use of eq. (4), see Figs. 3 and 4, creating a base for the calculation of "average, effective" crystal linear growth rate G values with the use of eq. (3). Selected kinetic results are presented in Table 1.

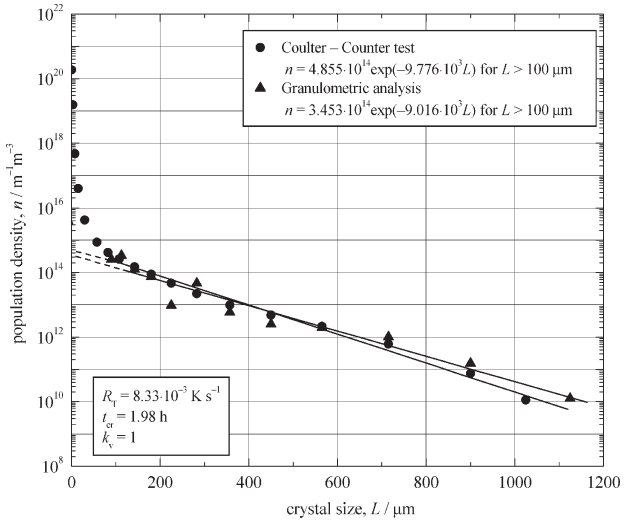

F i g . 3 – *Course of population density function ln n(L) of L(+)-ascorbic acid (LAA) crystals produced in a batch cooling crystallizer. Initial mass fractions in solution: LAA – 50, MeOH – 10, EtOH – 10, H_2O – 30 %. Comparison of population density values (n) calculated from mass CSD derived from particle laser analysis (Coulter counter) and from granulometric analysis.*

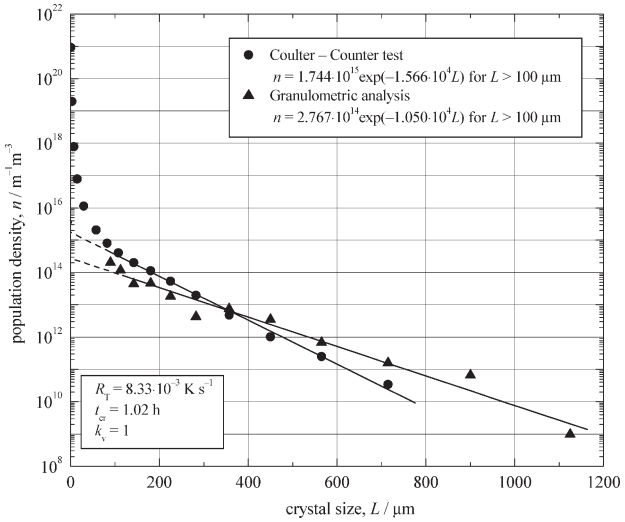

F i g . 4 – *Course of population density function ln n(L) of L(+)-ascorbic acid (LAA) crystals produced in a batch cooling crystallizer. Initial mass fractions in solution: LAA – 40, MeOH – 10, EtOH – 10, H_2O – 40 %. Comparison of population density values (n) calculated from mass CSD derived from particle laser analysis (Coulter counter) and from granulometric analysis.*

Results and discussion

Our own batch experimental data elaboration was preceded by statistical verification of the fundamental *Nývlt's* assumption (linearity in a "$z - L$" coordinate system, eqs. (1) and (2)). After application of the linear regression analysis it was concluded, that all R^2 values are within the 0.981 – 0.989 range, what practically confirms the usability of eqs. (1) and (2) for the investigated system (similar procedure is presented by *Freitas* and *Giulietti*[9]), warranting application of SIG kinetic model of a continuous MSMPR crystallizer, eq. (3), for the own batch experimental data elaboration. The calculation results are presented in Table 1.

It can be concluded, that with the increase in LAA mass fraction (w_{LAA}) in a LAA–MeOH–EtOH–H_2O system the metastable zone width decreases.[21] This phenomenon is not advantageous in continuous mass crystallization processes, restricting the range of sustainable distribution of supersaturation between two principal, competing processes of nucleation and growth, thus guarantying kinetic conditions for the stable enlargement of crystal sizes. Contrary, in a batch mode lowering of these boundaries influences the overall process course advantageously since it provides the desirable nucleation event within a shorter time, thus gives a convenient possibility of effective discharging of the generated supersaturation as it comes. This way reduction of

T a b l e 1 – *Influence of selected process parameters on the mass crystallization of LAA in a DT batch cooling crystallizer*

No.	w_{LAA} %	$R_T \cdot 10^3$ K s^{-1}	Metastable zone width[22]			t_{cr} h	Statistical parameters of CSD			Growth rate	
			T_s K	ΔT_{max} K	Δw_{max} %		L_m [a] mm	CV [a] %	L_m [b] mm	$G \cdot 10^8$ [a] m s^{-1}	$G \cdot 10^8$ [b] m s^{-1}
1	40	8.33	335	29	15.3	1.02	0.214	62.2	0.282	1.74	2.59
2	40	16.66	335	37	19.5	0.50	0.137	80.5	0.268	3.94	4.68
3	45	8.33	343	22	11.6	1.52	0.339	46.7	0.384	1.41	1.89
4	45	16.66	343	28	14.8	0.78	0.301	63.4	0.332	2.98	3.18
5	50	8.33	353	18	9.5	1.98	0.448	31.0	0.471	1.43	1.56
6	50	16.66	353	24	12.6	1.02	0.406	51.7	0.447	2.86	3.02

Mass fractions of alcohols in a raw material: MeOH – 10, EtOH – 10 %; distilled water – a complement to 100 %

a) Particle size analyzer COULTER LS-230

b) Granulometric analysis (PN–67/M-94001)

probability of uncontrolled homogeneous nucleation is possible. In practice it leads to more stable conditions of crystals growth, effecting in production of larger particles of higher quality.

Linear cooling rate, R_T, influences the process course considerably, as well. For $R_T = 8.33 \cdot 10^{-3}$ K s^{-1} increases in w_{LAA} from $w = 40$ to 45 and from $w = 45$ to 50 % correspond to reductions in ΔT_{max} equal 7 and 4 K, respectively. For $R_T = 16.66 \cdot 10^{-3}$ K s^{-1} the same increases in w_{LAA} give slightly higher reductions in ΔT_{max}, *i.e.*, 9 and 4 K.

Increase in w_{LAA} from 40 to 50 % corresponds thus to Δw_{max} reduction from 15.3 to 9.5 % for $R_T = 8.33 \cdot 10^{-3}$ K s^{-1} while for $R_T = 16.66 \cdot 10^{-3}$ K s^{-1} it corresponds to a decrease in Δw_{max} from 19.5 to 12.6 %. It should be generally noted, that higher values of cooling rate correspond to higher ΔT_{max} and Δw_{max} values.

It should be mentioned here, that in the system under study, considering the possibility of relatively high supercooling (supersaturation) existence, seed procedure is commonly applied to effectively reduce the metastable zone width in industrial, thus in a design-oriented laboratory-scale conditions. This way secondary nucleation mechanism, induced by the seeding solute crystals, enables one to induce the spontaneous formation of nuclei at the supersaturation level significantly lower than that corresponded to a primary homogeneous or – more likely – heterogeneous nucleation. Catalytic effect of seeds can be theoretically explained by the resulting effect of the following mechanisms: initial breeding, needle breeding, collision breeding, attrition, contact nucleation and fluid shear.

With w_{LAA} value increase an enlargement in a necessary batch crystallization time is also observed. Increase in w_{LAA} from $w = 40$ to 50 % corresponds to increase in crystallization time t_{cr} from 1.02 to 1.98 h ($R_T = 8.33 \cdot 10^{-3}$ K s^{-1}). For higher $R_T = 16.66 \cdot 10^{-3}$ K s^{-1} it corresponds to t_{cr} enlargement from 0.50 to 1.02 h. Linear correlations between w_{LAA} and t_{cr} are clearly observable. On the other hand a twofold increase in linear cooling rate produces, approximately, also twofold decrease in batch crystallization time for any w_{LAA} value tested. For $w_{LAA} = 40$ % increase in R_T from $8.33 \cdot 10^{-3}$ to $16.66 \cdot 10^{-3}$ K s^{-1} corresponds to a decrease in t_{cr} from 1.02 to 0.50 h, for $w_{LAA} = 45$ %: $t_{cr} = 1.52 \rightarrow 0.78$ h and for $w_{LAA} = 50$ %: $t_{cr} = 1.98 \rightarrow 1.02$ h.

Analysis of the changes in coefficient of variation, CV (where parameter CV is defined as standard deviation/mean size) suggests that doubling the linear cooling rate value while assuming other process parameter values constant produces in effect increase in CV value, in particular: CV = 62.2 → 80.5 % (by ca. 30 %) for $w_{LAA} = 40$ %, CV = 46.7 → 63.4 % (by ca. 36 %) for $w_{LAA} = 45$ % and CV = 31.0 → 51.7 % (by ca. 67 %) for $w_{LAA} = 50$ %. At the same time a clear decrease in mean LAA crystal size is observed, namely: $L_m = 0.214 \rightarrow 0.137$ mm (by ca. 36 %) for $w_{LAA} = 40$ %, $L_m = 0.339 \rightarrow 0.301$ mm (by ca. 11 %) for $w_{LAA} = 45$ % and $L_m = 0.448 \rightarrow 0.406$ mm (by ca. 9 %) for $w_{LAA} = 50$ %. The observed effects can be explained theoretically by relatively milder, more convenient conditions of mass transfer while generation and instant discharge of supersaturation in case of lower R_T value.

Combination in trends of change of these both process indicators suggests also, that two essential, superimposing phenomena can be responsible for the final results observed. Increase in homogeneous (locally) and heterogeneous nucleation rates results from a more intensive generation of supersaturation (higher cooling rate), producing also higher values of "effective" crystal growth rate: $G = 1.74 \cdot 10^{-8} \rightarrow 3.94 \cdot 10^{-8}$ m s^{-1} for $w_{LAA} = 40$ %, $G = 1.41 \cdot 10^{-8} \rightarrow 2.98 \cdot 10^{-8}$ m s^{-1} for $w_{LAA} = 45$ % and $G = 1.43 \cdot 10^{-8} \rightarrow 2.86 \cdot 10^{-8}$ m s^{-1} in case of $w_{LAA} = 50$ %. However, higher kinetic sensitivity of nucleation is expected. Contribution of theoretically possible interactions between imperfect crystal structure resulting from too high growth rates and intensification of secondary nucleation, *e.g.* needle breeding or polycrystalline breeding mechanisms can not be excluded (see electron microscope images in the work of *Wierzbowska et al.*[21]). Statistical characteristics of crystal suspension produced in these conditions (composed mainly of crystal fines) indicates both increase in crystal size dispersion (higher CV values) and effective decrease in mean crystal size, L_m. For a lower cooling rate applied mean crystal size is definitely higher, in spite of nearly two-times longer batch time what undoubtedly influences combined attrition, abrasion and breakage actions. It can be expected, that milder process conditions are of decisive influence, providing more stable and more convenient distribution of supersaturation.

An interesting phenomenon can be observed – for $w_{LAA} = 45$ and 50 % the values of crystal linear growth rate are nearly identical for the same values of linear cooling rate, R_T: $G = 1.41 \cdot 10^{-8}$ and $1.43 \cdot 10^{-8}$ m s^{-1} ($R_T = 8.33 \cdot 10^{-3}$ K s^{-1}) and $G = 2.98 \cdot 10^{-8}$ and $2.86 \cdot 10^{-8}$ m s^{-1} ($R_T = 16.66 \cdot 10^{-3}$ K s^{-1}). Considerably higher values were, however, observed for $w_{LAA} = 40$ %: $G = 1.74 \cdot 10^{-8}$ m s^{-1} ($R_T = 8.33 \cdot 10^{-3}$ K s^{-1}) and $G = 3.94 \cdot 10^{-8}$ m s^{-1} ($R_T = 16.66 \cdot 10^{-3}$ K s^{-1}). For the kinetic data elaborated on the basis of sieve analysis results the observed trends and qualitative conclusions are identical.

The values of crystal linear growth rate observed in a batch process under study are of the

same order as the values presented by *Freitas* and *Giulietti*:[9] $G = 1.26 \cdot 10^{-8} – 8.38 \cdot 10^{-8}$ m s^{-1} ($R_T = 2.78 \cdot 10^{-5} – 13.89 \cdot 10^{-5}$ K s^{-1}), $L_m = 0.123 \cdot 10^{-3} – 0.297 \cdot 10^{-3}$ m, batch time range $t_{cr} = 0.45 – 5.92$ h, maximal supercooling range $\Delta T_{max} = 6.9 – 26.8$ K and saturation temperature range $T_s = 321.3 – 334.9$ K. Lower values of ΔT_{max} should be related to lower (even by two orders of magnitude) values of linear cooling rate, R_T. Also *Omar*[1] in a seeded (6.25 g mass of seed crystals of $L_s = 250$ μm size) batch crystallization experiments reported similar results: in a pure water solution of LAA $G = 2.4 \cdot 10^{-8} – 5.4 \cdot 10^{-8}$ m s^{-1}, in a solution composed of w = 80 % water / w = 20 % ethanol $G = 2.4 \cdot 10^{-8} – 1.31 \cdot 10^{-7}$ m s^{-1}, in a solution composed of w = 80 % water / w = 20 % methanol $G = 1.20 \cdot 10^{-8} – 3.37 \cdot 10^{-7}$ m s^{-1} and in a solution composed of w = 80 % water / w = 20 % propanol $G = 8.17 \cdot 10^{-9} – 4.68 \cdot 10^{-7}$ m s^{-1}.

Considering simultaneous, complex action of two alcohols, crystal linear growth rate G was correlated with either solubility temperature of a batch mixture, T_s (Fig. 5) or a batch crystallization time, t_{cr} (Fig. 6). Various proportions in these both alcohols can produce identical effects, externally conveniently represented indirectly by T_s or t_{cr} parameters, both being complex functions of w_{LAA}, w_{MeOH}, w_{EtOH} – contrary to a case of only one alcohol's influence, where its concentration is an unequivocal factor influencing directly kinetic behavior of these systems.

It is observable, that CSD derived from sieve analysis data provides higher values of mean crystal

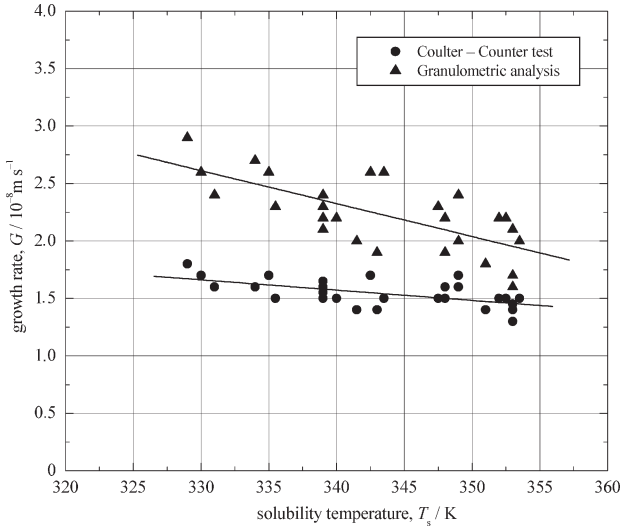

F i g . 5 – *Influence of solubility temperature, T_s, on the "average, effective" linear growth rate, G, of L(+)-ascorbic acid (LAA) crystals in a LAA–MeOH–EtOH–H_2O system (cooling rate $R_T = 8.33 \cdot 10^{-3}$ K s^{-1}). Comparison of G values calculated on the basis of CSDs derived from particle laser analysis (Coulter counter) and from granulometric analysis (see Table 1 for details).*

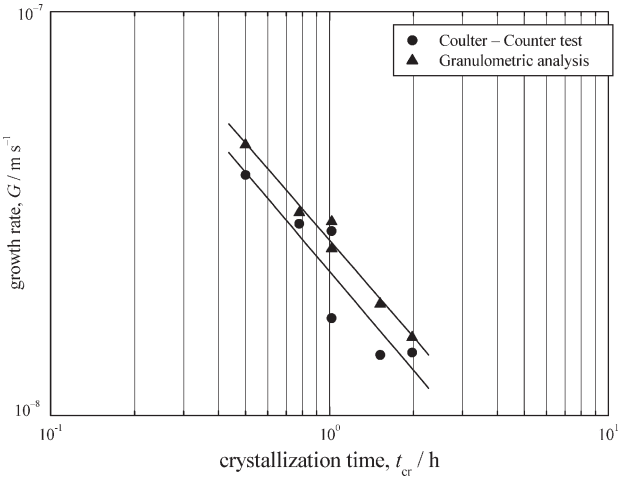

F i g . 6 – *Influence of batch crystallization time, t_{cr}, on the "average, effective" linear growth rate, G, of L(+)-ascorbic acid (LAA) crystals in a LAA–MeOH–EtOH–H_2O system – eqs. (6) and (7) (two linear cooling rates: $R_T = 8.33 \cdot 10^{-3}$ K s^{-1} and $R_T = 16.66 \cdot 10^{-3}$ K s^{-1} and three LAA mass fractions: w = 40, 45 and 50 % considered, see Table 1 for details).*

size, L_m (see Table 1). Linear crystal growth rate, G, values calculated on the basis of this CSD have thus overstated values, what should be related to the course of linear segment of ln $n(L)$ dependency (see Figs. 3 and 4). These overstated values of population density, n, compared to the n recalculated from Coulter counter data result from specificity of granulometric analysis procedure, where theoretically exists a possibility of retention of particles of a size lower than mesh dimension, *e.g.* in case of clogging-up of the sieve meshes. Moreover, an essential problem seems to be the influence of non-isomerism of particles and diversity in their cross-dimension values. A possibility of undergoing through the meshes depends on its momentary, accidental configuration in space. This effect is distinctly observed for the elongated particles, like needle-shape LAA crystals[21] – see scanning electron microscope images in Fig. 7.

In case of laser particle analysis (Coulter counter) accidental exposition of non-isomeric particle with respect to a detector's light ray is of primary importance. Other possible problems arise from taking into consideration individual volumes of particles. Granulometric analysis provides *de facto* determination of mass (volume) distribution of a crystal population, while laser analysis provides its specific surface area distribution. Problems resulting from distinctness between analytical procedures applied are further described in a work of *Mora et al.*,[41] where some relations for a direct comparison of CSD data derived from both discussed sources are also presented and explained in detail.

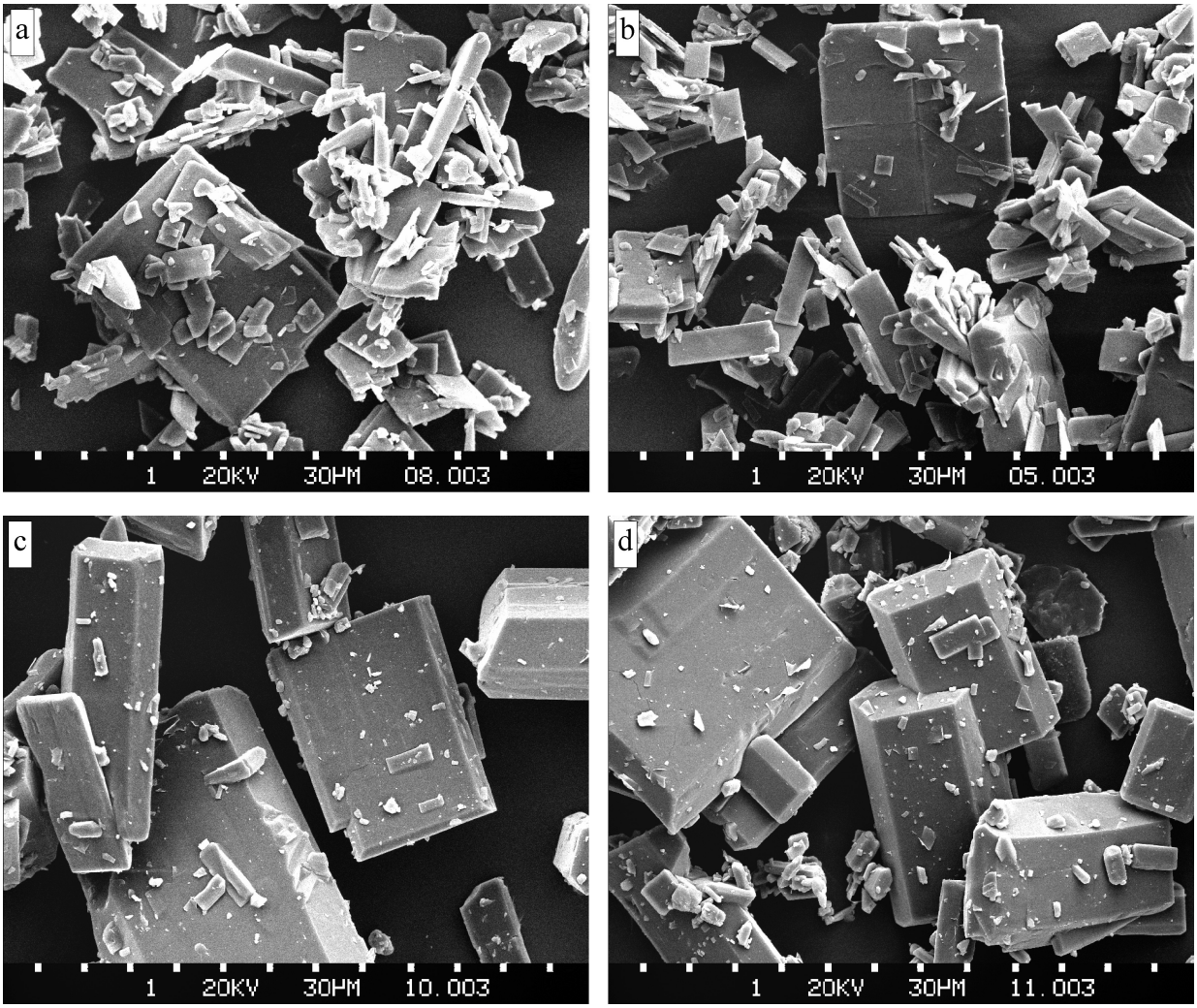

F i g . 7 – *Scanning electron microscope images (magnification: 300x) of L(+)-ascorbic acid (LAA) crystals produced in a LAA–MeOH–EtOH–H_2O system (DT batch cooling crystallizer): (a) test No. 1, (b) test No. 2, (c) test No. 5, (d) test No. 6 – see the data in Table 1*

The resulting kinetic equations in a $G = f(t_{cr})$ form (see Fig. 6), depending on analytical method used for CSD determination, can be presented as empirical correlations, eqs. (6) and (7):

$$G = 1.80 \cdot 10^{-5} t_{cr}^{-0.815} \qquad (R^2 = 0.913) \qquad (6)$$

or:

$$G = 1.87 \cdot 10^{-5} t_{cr}^{-0.798} \qquad (R^2 = 0.988) \qquad (7)$$

where: t_{cr} – batch crystallization time (s), defined in general by eq. (5) or, for the particular system under study, by eq. (5a). An $G = f(t_{cr})$ equation is the most general form since t_{cr} is an indirect function of, among others, T_{cr}, where $T_{cr} = T_s - \Delta T_{max}$.

Eq. (6) is based on the G values calculated from CSDs (in a form of population density functions) derived from laser particle size analyzer COULTER LS–230, whereas eq. (7) – on the ones from granulometric analysis data. After critical comparison of these two equations it results, that the influence of batch time on the G values is practically identical (see the exponent values in eqs. (6) and (7) as ca. –0.8). Since from granulometric analysis data one obtains overestimated values of the CSD parameters (compare L_m values in Table 1), laser analysis results, eq. (6), are recommended by the authors as more reliable. For the case under study eq. (6) can be further rearranged to the following, detailed form of eq. (6a):

$$G = f(w_{LAA}, w_{MeOH}, w_{EtOH}, T_f, R_T, t_f) = 1.180 \cdot 10^{-5} \cdot \left[\frac{2.932 w_{LAA} + 0.671 w_{MeOH} + 0.883 w_{EtOH} + 174.78 - T_f}{R_T} + t_f \right]^{-0.815} \qquad (6a)$$

From the presented equation it becomes possible to determine an "average, effective" value of crystal linear growth rate, G, in a batch process ac-

cording to the *Nývlt's* concept. If the profiles of supersaturation discharge during process time are identical in character (or similar, *e.g.* as parallel curves) in a set of batch experiments (however, for the diversified sets of other process parameter values) it may be – theoretically – possible to use this relative, conventional growth rate as an entirely nominal parameter, convenient for, at least rough, comparative analysis purposes.[34]

Conclusions

Selected kinetic aspects of crystal growth in a batch, polythermic, isohydrical and seeded process of vitamin C (LAA) mass crystallization from water-alcohols mixtures were raised and discussed. Kinetic model describing mass crystallization process in a continuous, physically idealized MSMPR apparatus, mathematically convenient for the kinetic data determination was formally adopted, after positive verification of the *Nývlt's* assumptions and restrictions, to the batch process under study. Size-independent growth (SIG) kinetics was assumed.

It can be concluded that the largest (L_m) and more uniform (CV) particles of purified, crystalline vitamin C correspond to higher initial fraction of LAA in a solution (w_{LAA}) and lower cooling rate (R_T) applied, what is connected with the elongation of batch crystallization time (t_{cr}). An observed difference between the extreme L_m values is ΔL_m = 0.448 – 0.137 = 0.311 mm (Coulter counter data) or ΔL_m = 0.471 – 0.268 = 0.203 mm (granulometric analysis data) while the difference between CV values is ΔCV = 80.5 – 31.0 = 49.5.

Because of the considerable, fundamental differences in the batch and continuous process regimes the resulting kinetic data should be – according to the *Nývlt's* concept – of formal meaning only, *e.g.* as a convenient calculation parameter, however providing one with the quantitative characterization of a complex batch, seeded and polythermic process of simultaneous nucleation and crystals growth precisely enough for the engineering design in a form of "average, effective kinetic parameter" values. Moreover, application of this formal approach enables one to make a more objective comparison plane between the kinetic datasets derived from both continuous and batch mass crystallization processes, *e.g.* in a technology of vitamin C purification.

Comparing own experimental results with *Freitas* and *Giulietti*[9] as well as *Omar*[1] data it can be concluded, that these are of the same magnitude. Observed diversification results probably from different experimental conditions and/or laboratory measurement accuracy. It is worth to mention, that in the process conditions providing relatively low crystal growth rates batch regime secures a more efficient control resulting in larger crystals formation, additionally of lower size dispersion (CV) than it can be obtained in a continuous MSMPR crystallizer.[38,42] Thus, the experimental data presented, together with their specific and restricted kinetic interpretation according to the *Nývlt's* concept as an "average, effective" G value estimation and correlated in a form of empirical kinetic equation $G(t_{cr}$, *other technological parameters*…) can find practical application in the design and/or optimization of modern technologies of LAA purification on the way of multistage batch mass crystallization processes.

ACKNOWLEDGEMENTS

This work was supported by the Scientific Research Committee (Ministry of Science and Higher Education of Poland) under grant No. 3T09B 122 27.

LAA crystal size distributions were measured by means of particle size analyzer COULTER LS–230 in the Institute of Inorganic Chemistry, Gliwice, Poland.

Images of LAA crystals (scanning electron microscope JEOL–5800 LV) were made in Head of Materials Science Laboratory of the Institute of Materials Science and Applied Mechanics, Wroclaw University of Technology, Wroclaw, Poland.

List of symbols

- d – draft tube diameter, m
- d_m – agitator diameter, m
- D – crystallizer diameter, m
- G – average, effective linear growth rate of crystals, m s^{-1}
- h – draft tube height, m
- h_p – vertical distance between propeller agitator level and crystallizer bottom, m
- H – crystallizer height, m
- k_F – surface shape factor of crystal
- k_v – volumetric shape factor of crystal
- L – crystal characteristic size, m
- L_i – mean size of i-th crystal fraction, m
- L_m – mean size of crystal population, m
- L_s – seed size, m
- ΔL_i – size range width of i-th crystal fraction, m
- m_i – mass of i-th crystal fraction, kg
- n – population density (number of crystals within the defined size range divided by this size range width per unit volume of suspension), m^{-1} m^{-3}

n_i – population density of *i*-th crystal fraction, m^{-1} m^{-3}

n_0 – population density of nuclei (zero-size crystals), m^{-1} m^{-3}

N – agitator's revolution number, s^{-1}

q_v – volumetric flow rate of crystal suspension, m^3 s^{-1}

R^2 – correlation coefficient

R_T – linear cooling rate, K s^{-1}

t_{cr} – batch crystallization time, s

t_f – time of stabilization of the resulting postprocessing suspension in a final batch process temperature, s

T – temperature, K

T_{cr} – temperature of spontaneous LAA nucleation, K

T_f – final temperature of batch crystallization process, K

T_s – LAA solubility temperature, K

ΔT_{max} – critical, maximal value of supercooling in the solution (maximum allowable supercooling), defined as $T_s - T_{cr}$, K

V_i – volume of the *i*-th crystal fraction, m^3

V_t – total volume of crystallizer, m^3

V_w – working volume of crystallizer, m^3

W – normalized cumulative mass distribution (undersize)

w – mass fraction, %

w_{EtOH} – initial mass fraction of ethanol in solution, %

w_{LAA} – initial mass fraction of L(+)-ascorbic acid (LAA) in solution, %

w_{MeOH} – initial mass fraction of methanol in solution, %

Δw – supersaturation of LAA in solution, %

Δw_{max} – critical, maximal supersaturation of LAA in solution, %

z – dimensionless size

Greek letters

ρ – crystal density, kg m^{-3}

τ – mean residence time of crystal suspension, defined as V_w/q_v, s

Abbreviations

CSD – crystal size distribution

CV – coefficient of variation (of crystal sizes), %

DT – draft tube (crystallizer type)

EtOH – ethanol

LAA – L(+)-ascorbic acid (vitamin C)

MeOH – methanol

MSMPR – mixed suspension mixed product removal (crystallizer type)

SIG – size-independent growth (kinetics)

References

1. *Omar, W.*, Chem. Eng. Technol. **29** (1) (2006) 119.
2. *Omar, W.*, *Ulrich, J.*, Cryst. Res. Technol. **41** (5) (2006) 431.
3. *Reichstein, T.*, *Grussner, A.*, Helv. Chim. Acta **17** (1934) 311.
4. *Boudrant, J.*, Enzyme Microb. Technol. **12** (1990) 322.
5. *Šnajdman, L. O.*, Proizvodstvo Vitaminov, Piscevaja Promyšlennost, Moskva, 1973 (in Russian).
6. *Bodor, B., Halasz, S., Vassanyi, I.,* Crystallization parameters influencing size, habit and purity of vitamin C, in: Proceedings of the 12th Symposium on Industrial Crystallization, Rojkowski, *Z. H.* (Ed.), Warsaw, Poland, 1993, 4.065.
7. *Bodor, B., Dodony, I.,* Hung. J. Ind. Chem. **23** (1995) 289.
8. *Bodor, B., Lakatos, B. G.*, Hung. J. Ind. Chem. **27** (1999) 297.
9. *Freitas, A. M. B., Giulietti, M.*, Crystallization of L-ascorbic acid from aqueous solutions, in Proceedings of the 15th Symposium on Industrial Crystallization, *Angelo Chianese* (Ed.), Sorrento, Italy, 2002, No. 232 (CD–ROM).
10. *Matynia, A., Wierzbowska, B., Bechtold, Z., Kozak, E.*, Nucleation of vitamin C, in Proceedings of the 14th Symposium on Industrial Crystallization, Inst. of Chem. Engineers (Ed.), Cambridge, England, 1999, No. 0090 (CD–ROM).
11. *Davies, M. B., Austin, J., Partridge, D.*, Vitamin C: Its Chemistry and Biochemistry, The Royal Society of Chemistry, Cambridge, 1991.
12. *Taqui, M. M., Martell, A. E.,* J. Am. Chem. Soc. **89** (1967) 4176.
13. *Hajratwala, B. R.*, STP Pharma **1** (4) (1985) 281.
14. *Fyhr, P., Brochin, A.*, Acta Pharm. Suec. **24** (1987) 15.
15. *Halasz, S., Bodor, B.*, J. Cryst. Growth **128** (1993) 1212.
16. *Angberg, M., Nystrom, C., Cantesson, S.*, Internat. J. Pharm. **90** (1) (1993) 19.
17. *Smirnov, N. J., Streltsov, V. V., Zarucki, V. V., Suprunov, N. A.*, Izv. Vyssh. Uchebn. Zaved. Khim. Khim. Tekhnol. **18** (1975) 126 (in Russian).
18. *Suprunov, N. A., Lymar, A. P., Varentsov, V. V., Streltsov, V. V., Smirnov, N. J.*, Massov. Kristall. **3** (1994) 45 (in Russian).
19. *Matynia, A., Wierzbowska, B., Bechtold, Z.*, Inz. Ap. Chem. **37** (6) (1998) 3 (in Polish).
20. *Matynia, A., Wierzbowska, B., Szewczyk, E.*, Pol. J. Chem. Technol. **2** (1) (2000) 14.
21. *Wierzbowska, B., Matynia, A., Piotrowski, K., Koralewska, J.*, Chem. Eng. Proc. **46** (2007) 351.
22. *Myerson, A. S.,* Handbook of Industrial Crystallization, Butterworth–Heinemann, Stoneham, MA, 1993.
23. *Liu, Y., Wang, J. K., Wie, H. Y.*, J. Cryst. Growth **271** (2004) 238.
24. *Fevotte, M. G., Hoff, C., Klein, J. P.*, Chem. Eng. Sci. **52** (1997) 1125.
25. *Sahin, Ö., Özdemir, H., Kendirci, N., Balatca, A.*, J. Cryst. Growth **219** (2000) 75.
26. *Aoun, M., Plasari, E., David, R.*, Chem. Eng. Sci. **54** (1999) 1161.
27. *Qiu, Y., Rasmuson, A.*, Chem. Eng. Sci. **46** (1991) 1659.
28. *Qiu, Y., Rasmuson, A.*, AIChE J. **36** (1990) 665.
29. *Halfon, A., Kaliaguine, S.*, Can. J. Chem. Eng. **54** (1976) 160.
30. *Tavare, N. S., Garside, J.*, Chem. Eng. Res. Des. **64** (1986) 109.

31. *Witkowski, W. R., Miller, S. M., Rawlings, J. B.*, ACS Symp. Ser. **438** (1990) 102.
32. *Yokota, M., Sato, A., Kubota, N.*, Chem. Eng. Sci. **55** (2000) 717.
33. *Nývlt, J., Söhnel, O., Matuchová, M., Broul, M.*, The Kinetics of Industrial Crystallization, Academia, Praha, 1985.
34. *Garside, J., Mersmann, A., Nývlt, J.*, Measurement of Crystal Growth Rate, European Federation of Chemical Engineering – Working Party on Crystallization, München, 1990.
35. *Randolph, A. D., Larson, M. A.*, Theory of Particulate Processes, Academic Press, New York, 1988.
36. *Mullin, J. W.*, Crystallization, Butterworth – Heinemann, Oxford, 1992.
37. *Rojkowski, Z., Synowiec, J.*, Crystallization and Crystallizers, WNT, Warszawa, 1991 (in Polish).
38. *Mersmann, A. (Ed.)*, Crystallization Technology Handbook, Marcel Dekker, New York, 1995.
39. *Wierzbowska, B., Matynia, A., Cwiertnia, E., Bechtold, Z.*, Inz. Ap. Chem. **43** (4/5) (2004) 48 (in Polish).
40. *Paul, E. L., Tung, H.–H., Midler, M.*, Powder Technol. **150** (2005) 133.
41. *Mora, C. F., Kwan, A. K. H., Chan, H. C.*, Cement and Concrete Research **28** (1998) 921.
42. *Moyers, J. R., Rousseau, R. W.,* in: Handbook of Separation Processes, *Rousseau R. W.* (Ed.), Wiley, New York, 1987.